Extended Abstracts of the 2003 International Conference on Solid State Devices and Materials, Tokyo, 2003, pp. 874-875

F-8-1 (Invited)

Semiconductor Photonic Crystal Devices

Toshihiko Baba

Yokohama National University, Dept. Electr. & Computer Eng.
79-5 Tokiwadai, Hodogayaku, Yokohama 240-8501, Japan
Phone./Fax +81-45-339-4258, e-mail baba@ynu.ac.jp

Semiconductor photonic crystals are expected to realize various novel performance and functions in photonic devices, e.g. ultralow threshold lasing in nanolasers,[1-3] high efficiency light extraction from LEDs,[4] flexible optical wirings by ultrasmall waveguide elements,[5-7] unique light localization and radiation in defects,[8] high resolution filtering and wide angle deflection of light by the superprism phenomenon,[9-11] and strong nonlinear response by an ultrasmall group velocity of light at a photonic band-edge.[12] They have been theoretically investigated and partly demonstrated in the experiment. Most popular structures in the experiment are the photonic crystal slab as a 2-D crystal[1-3,5-8] and the woodpile structure as a 3-D crystal.[13-15]

The photonic crystal slab is a semiconductor membrane with an array of airholes, as shown in Fig. 1. The structure allows the strong optical confinement for the in-plane polarization by the photonic bandgap in the in-plane direction and by the total internal reflection in the vertical direction. The typical material is Si for passive devices and GaInAsP (λ_g = 1.55 μm) for active devices, both of which have a high refractive index of 3.1 – 3.5. The thickness and airhole diameter are both 0.2 – 0.3 μm. These values are determined by the perfect optical confinement condition that at least one photonic band exists below the light line in the 3-D photonic band diagram, which is the boundary of pure guided and radiation modes. In the fabrication, we use ICP etching for the hole opening and the selective wet chemical etching of sacrificial layers. The etching process for holes with an aspect ratio of 1.0 is relatively easy. The introduction of point and line defects is also simple in the lithographic process. These defects maintain the localized and guided modes, respectively, which can be used for nanolasers and waveguides.

So far, the room temperature pulsed lasing by photopumping has been achieved in some groups for such photonic crystal nanolasers with a simple point or line defect in a triangular or square lattice. However, the defect does not necessarily have such simple shapes. The photonic bandgap allows a localized mode in arbitrary defects. The lasing can also occur at a bend, a branch and an intersection of line defects, as shown in Fig. 2. Point and line composite defects are other candidates. Thus the photonic crystal provides large design flexibility for lasers in photonic crystal integrated circuits. The photonic crystal waveguide has been improved in these years by using the Si technology for the SOI substrate. Due to the high refractive index contrast boundaries and the ultrasmall channel core, the light scattering loss is still higher than 1 dB/mm.

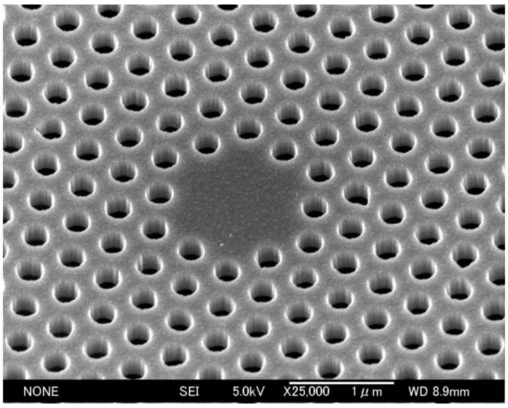

(a)

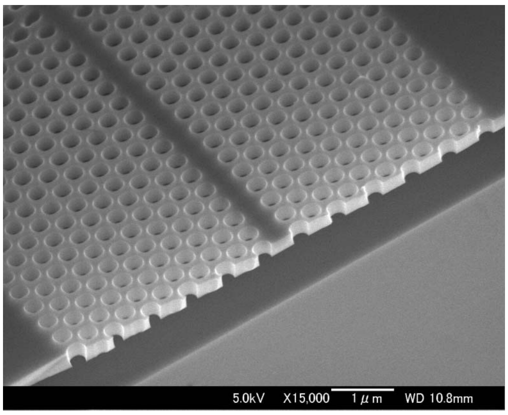

(b)

Fig. 1 Photonic crystal slab devices. (a) GaInAsP point defect (H2) laser. (b) Si single line defect waveguide.

But this value seems to be low enough for actual applications since small waveguide elements, e.g., small bends, branches and directional couplers, and the small group velocity drastically miniaturize the size of the photonic circuit.

Anomalous light propagation characteristics of photonic crystals at light-conductive frequencies provide a large angular dispersion called the super-prism phenomenon,[9] which can be used as a diffraction-type optical filter with a Gaussian frequency response and as a deflector of light beam.[11] To optimize the structure and the width and angle of the incident beam, the dispersion surface and corresponding wavelength resolution parameters $(\partial\theta_c/\partial(a/\lambda))/(\partial\theta_c/\partial\theta_{in})$ were analyzed over the Brillouin zone,[10] where θ_c and θ_{in} are beam angle in the crystal and in the incident medium, respectively, and a is the lattice constant. The result showed that the beam divergence $\partial\theta_c/\partial\theta_{in}$ of photonic crystals strongly restricts the optimum condition; it requires the incident beam to be >100 μm wide and makes the photonic crystal to be of cm order. To avoid this problem, we propose a new superprism which utilizes anomalous characteristics of the ***k***-vector and an angled output end of the crystal. We named it ***k**-vector superprism*. According to the same analysis, as shown in Fig. 4, this type of prism will drastically reduce the size of the photonic crystal to be of 10 μm order, keeping a high resolution. It also allows an incident beam of less than 20 μm in width. Issues are optimizations of input and output ends of the crystal, which ensure a high transmission efficiency and of a lens outside the photonic crystal, which shortens the total filter system.

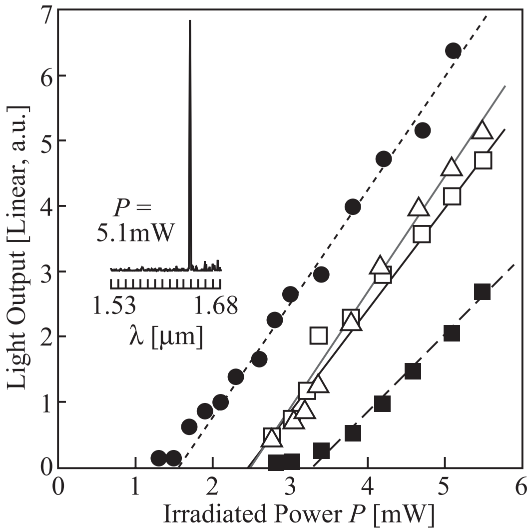

Fig. 2 Lasing characteristics of photonic crystal lasers at room temperature. Open triangle and square denote 60º bend and Y-branch, respectively. Closed square and circle denote line defect and H7 point defect, respectively. The spectrum is for H7 defect.

The fabrication of a 3-D photonic crystal is still a challenging research. But the manipulation technique of semiconductor micro-parts proposed by RIKEN is unique and promising for constructing the woodpile structure with sufficient layer numbers and arbitrary defects, as shown in Fig. 3.[15] The photonic bandgap was confirmed at λ = 3 – 5 μm. We expect that this method is applied to a practical field by developing an automatic assembly technique.

References

1. O. Painter, R. K. Lee, A. Scherer, A. Yariv, J. D. O'Brien, et al., Science **284**, 1819 (1999).
2. A. Sugitatsu and S. Noda, Electron. Lett. **39**, 213 (2003).
3. K. Inoshita and T. Baba, Electron. Lett. **41** (2003, in press).
4. T. Baba and H. Ichikawa, Optoelectronic and Commun. Conf. 9C2-1 (2002).
5. T. Baba, N. Fukaya and J. Yonekura, Electron. Lett. **35**, 654 (1999).
6. J. Yonekura, M. Ikeda and T. Baba, J. Lightwave Technol. **17**, 1500 (1999).
7. T. Baba, A. Motegi, T. Iwai, et al., IEEE J. Sel. Top. Quantum Electron. **38**, 743 (2002).
8. S. Noda, et al., Nature **407**, 608 (2000).
9. H. Kosaka, T. Kawashima, A. Tomita, et al., Phys. Rev. B **58**, R10096 (1998).
10. T. Baba and T. Matsumoto, Appl. Phys. Lett. **81**, 2325 (2002).
11. T. Baba and M. Nakamura, IEEE J. Quantum Electron. **38**, 909 (2002).
12. T. Baba and T. Iwai, Jpn. J. Appl. Phys. **42**, 1603 (2003).
13. J. G. Fleming, et al., Opt. Lett. 24, **49** (1999).
14. S. Noda, K. Tomoda, N. Yamamoto, and A. Chutinan, Science **289**, 604 (2000).
15. K. Aoki, H. T. Miyazaki, H. Hirayama, K. Inoshita, et al., Nature Materials **2**, 117 (2003).